Available online at www.sciencedirect.com
ScienceDirect
Sensors and Actuators A 136 (2007) 723–729
SENSORS AND ACTUATORS A PHYSICAL
www.elsevier.com/locate/sna

Improvement of flow and pressure controls in diffusion-tube humidity generator: Performance evaluation of trace-moisture generation using cavity ring-down spectroscopy

Hisashi Abe*, Hiroshi Kitano

National Metrology Institute of Japan (NMIJ), AIST, AIST Tsukuba Central 3, Tsukuba 305-8563, Japan

Received 4 September 2006; received in revised form 23 October 2006; accepted 12 December 2006
Available online 20 December 2006

Abstract

A system of flow and pressure controls for a magnetic suspension balance/diffusion-tube humidity generator (MSB/DTG) has been developed to realize a humidity standard in the trace-moisture region. The system essentially consists of a pressure regulator combined with a piezo valve, and adopts a simple stepwise change in the total flow rate. It has been demonstrated that the uncertainty of evaporation rates is greatly reduced by applying buoyancy correction to mass data measured with the MSB. Using the system and buoyancy-corrected data, the negative effect on the MSB/DTG observed upon changing the total flow rate become negligible. The relative standard uncertainty of total flow rates is evaluated using mass flow meters composed of critical flow Venturi nozzles to be less than or equal to 0.22%. The uncertainty of humidity generation has been significantly reduced by improvements introduced in this work. A comparison between humidity generated with the DTG and humidity measured with a moisture analyzer (MA) based on cavity ring-down spectroscopy is presented in the amount-of-substance fraction range between 10 nmol/mol and 250 nmol/mol. The results of the comparison confirm that the DTG is capable of producing a trace-moisture gas down to approximately 10 nmol/mol, and of easily varying and controlling the amount-of-substance fraction of water using the system. The sources of bias observed in the MA reading are attributable mainly to systematic errors in the temperature of the absorption cell and absorption cross section used to calculate the water concentration with the MA.
© 2007 Elsevier B.V. All rights reserved.

Keywords: Humidity standard; Diffusion tube; Magnetic suspension balance; Trace moisture; Sensor calibration; Critical flow Venturi nozzle

1. Introduction

The measurement of trace impurities in process gases has become increasingly important in the past decade in semiconductor industries, because it has been recognized that impurities play a critical role in the yield and product quality of semiconductor devices. Water is a common impurity, and the level of control currently required is considered to be better than 1 μmol/mol in amount-of-substance fraction [1]. Various sensors have been developed to detect such a small amount of water vapor [2], and many of them are commercially available and commonly used in the fields of science and industry. However, the accurate measurement of trace moisture is not straightforward. A major reason behind this is the lack of suitable humidity standards for the calibration of sensors; the periodic calibration of sensors is needed to achieve reliable measurement.

In our previous study [3], it was demonstrated that a diffusion-tube humidity generator (DTG) is a suitable and reliable humidity standard in the trace-moisture region. The DTG generates humidity by mixing water vapor evaporated from a diffusion cell [3] with dry gas. Therefore, to establish a primary humidity standard with this method, it is necessary to measure and control the evaporation rate of the water and the flow rate of the gas. In the previous study, we developed a system for the real-time mass measurement of the evaporated water using a magnetic suspension balance (MSB) combined with the DTG. Furthermore, using a moisture analyzer (MA) based on cavity ring-down spectroscopy [4–6], it was shown that the stable generation of water evaporation is realized by precisely controlling temperature and pressure.

In this work, we focus on the measurement and control of flow rate. The water concentration of the humid gas generated

* Corresponding author.
E-mail address: abe.h@aist.go.jp (H. Abe).

0924-4247/$ – see front matter © 2007 Elsevier B.V. All rights reserved.
doi:10.1016/j.sna.2006.12.013

with the DTG can be varied by adjusting the total flow rate. This was performed using a mass flow controller (MFC) by adjusting the flow rate of the gas passing through the bypass line of the MSB/DTG. When the total flow rate is changed, we must not disturb the flow to the generation chamber of the MSB/DTG because of the need to maintain the weighing stability and sensitivity of the MSB. We must also maintain the pressure inside the chamber because of the need to realize a stable and constant evaporation rate. This pressure change also produces a change in the buoyancy acting on the diffusion cell, which would be a serious problem in real-time mass measurement with the MSB. In fact, disturbances in the flow and pressure were observed upon changing the total flow rate, and they brought about the problems mentioned above. To solve these problems, we have developed a system of flow and pressure controls using a pressure regulator combined with a piezo valve, and by adopting a stepwise change in the total flow rate.

The measurement of the total flow rate is a fundamental issue for determining the water concentration of humid gas generated with the DTG. In the present study, the rate was measured using mass flow meters (MFMs) composed of critical flow Venturi nozzles, which are often used as a transfer standard among national metrology institutes [7]. The uncertainty of the total flow rate has also been evaluated with the MFMs.

A comparison between humidity determined with the evaporation and flow rates and humidity measured with the MA is presented. The sources of the bias observed in the MA reading are discussed.

2. Experimental

2.1. Experimental setup

Fig. 1 shows a schematic of the experimental setup used in the present study. Two thermal mass flow controllers (Stec, SEC-F440M), referred to as MFC_1 and MFC_2, were used to control the flow of dry nitrogen (N_2) gas. The full scales of MFC_1 and MFC_2 were 20 L/min and 5 L/min, respectively; the flow rates used in this paper correspond to those measured under

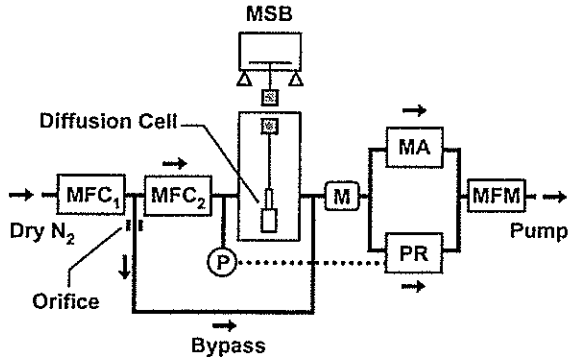

Fig. 1. Schematic of the experimental setup used in this work. MFC denotes the thermal mass flow controller, P is the pressure gauge, MSB is the magnetic suspension balance, M is the mixing device, PR is the pressure regulator, MA is the moisture analyzer based on cavity ring-down spectroscopy, and MFM is the mass flow meter composed of a critical flow Venturi nozzle.

the standard conditions of 101.325 kPa and 0 °C. The total flow rate of the system was controlled with MFC_1 in the range between 1 L/min and 20 L/min. A portion of the flow, at a rate of 0.10 L/min, was introduced to the inlet of a generation chamber using MFC_2, and the rest of the flow was bypassed. The flow to the bypass line was choked at the inlet of the line using an orifice to maintain sufficient pressure upstream of MFC_2 so that MFC_2 performed properly. A diffusion cell was suspended inside the chamber. The water vapor from the diffusion cell was diluted with the dry N_2 gas coming from the inlet. Humid gas obtained from the outlet of the chamber was mixed again with the bypassed flow. A mixing device (Noritake, Static mixer) was inserted after the connection point to achieve homogeneous mixing. This mixed flow was divided into two flows as below. One flow was introduced to a pressure regulator (PR) to control the pressure inside the chamber. The other flow was introduced to an MA based on cavity ring-down spectroscopy (Tiger Optics, MTO-1000) to monitor the amount-of-substance fraction of water in the trace-moisture gas generated. The flow to the MA was controlled with the built-in MFC of the MA. The MA probes the peak intensity of an absorption line of H_2O using a near-infrared diode laser. The deviation of the laser frequency from the peak is an uncertainty of the measurement. We confirmed that the uncertainty due to this effect in this work was negligible. The two flows were combined again after passing through the PR and MA. The flow rate of this combined flow was measured using one of two MFMs (Hirai, MR series), denoted MFM_1 and MFM_2, respectively. MFM_1 was used for flow rates greater than or equal to 10 L/min, and MFM_2 for those less than 10 L/min. The MFM consisted mainly of a temperature sensor, two pressure sensors, and a critical flow Venturi nozzle [8–10]. The Venturi nozzle produced a constant flow rate at its throat. Therefore, with a known cross-sectional area of the throat, the flow rate was calculated using the temperature and pressure of the gas measured upstream of the nozzle. The effect of leaks in the pipework on the measurement of flow rate was checked in advance and found to be negligible.

Evaporation rates were measured as the mass-change rates of the diffusion cell using the MSB. The mass data were collected every 1 min. The zero-point correction and calibration of the MSB were performed every 10 min and every 30 min, respectively. The details of the diffusion cell and the MSB were described in our previous paper [3]. The temperature of the chamber was maintained at 25 °C by monitoring the temperature with a platinum resistance thermometer (PRT). Atmospheric pressure was measured with a digital manometer (Yokogawa, MT210). Temperature and relative humidity near the MSB were measured with a PRT and a humidity sensor (Sato Keiryoki, SK-L200TH), respectively. The data of pressure, temperature, humidity, and flow rate were collected every 1 min using a personal computer.

2.2. Flow and pressure controls

A piezo actuator valve (Horiba Stec, PV-2000) combined with a valve controller (Horiba Stec, PCU-2100) was used to control the pressure inside the chamber at a constant value by

monitoring the absolute pressure with a pressure sensor (Pureron Japan, PC-305). In this work, the pressure was fixed to be 150 kPa. The proportional-integral-derivative (PID) parameters of the controller and MFC_2 were also tuned to minimize the effect of flow change on the pressure inside the chamber. In addition, a stepwise change in the total flow rate was adopted with MFC_1 upon the flow change. Each step of the flow change was 0.1 L/min. After a step, the flow rate was maintained at the new value for 3 s, and then changed to the next value. This procedure was repeated until the total flow rate became a desired value. The same computer as that described in Section 2.1 was also used to apply the stepwise control to MFC_1.

3. Results and discussion

3.1. Effect of flow change on MSB/DTG

First, we examine the effect of the total flow change on the MSB/DTG using the control system developed in this work. The total flow rate was changed alternately between 1 L/min and 20 L/min at intervals of 2 h as shown in Fig. 2(a). The pressure inside the chamber is shown in Fig. 2(b); the pressure disturbance in the figure is ±0.04 kPa. Fig. 2(c) shows the change in mass of the diffusion cell. The values of the mass data are the differences from the initial mass. The mass-change rate was determined to be 12.09(0.01) $\mu g\,h^{-1}$ using a least-squares fitting of the mass data with a linear function, where the number in parenthesis is the numerical value of the standard uncertainty [11] of the line fitting. The residuals of the fit are presented at the bottom of the figure on a 10× expanded scale. The observed

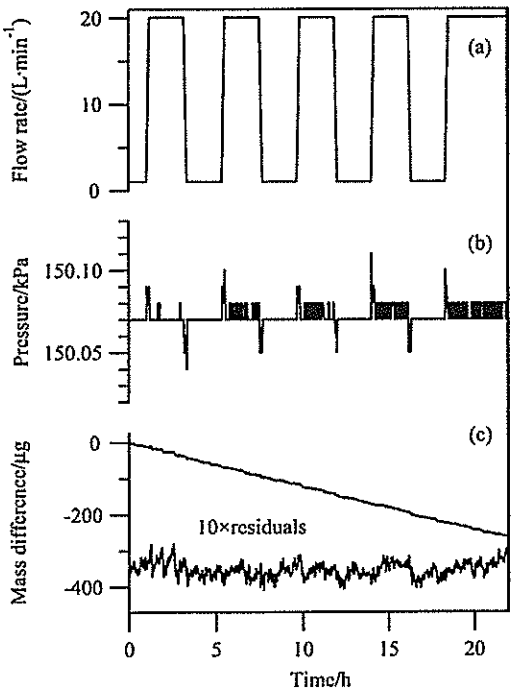

Fig. 2. Effect of total flow change on MSB/DTG: (a) total flow rate was changed alternately between 1 L/min and 20 L/min at intervals of 2 h; (b) pressure inside chamber; (c) change in mass of diffusion cell measured with MSB. The residuals of the fit are presented at the bottom on a 10× expanded scale.

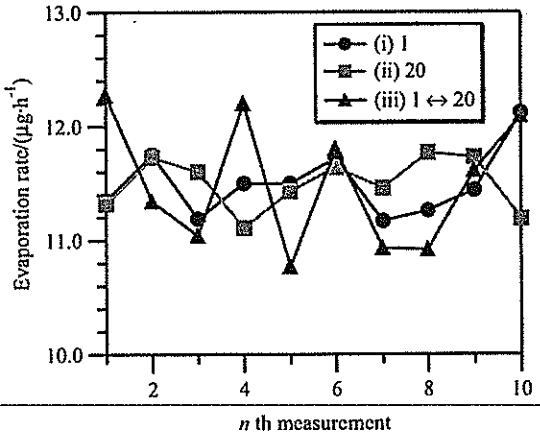

Fig. 3. Mass-change rates measured under three different flow control conditions as follows: (i) total flow rate was maintained at 1 L/min, (ii) maintained at 20 L/min, and (iii) changed alternately between 1 L/min and 20 L/min at intervals of 2 h.

mass data are reproduced very well by the linear function. This suggests that the effect of the total flow change on the weighing stability of the MSB seems to be negligible. However, it is possible that there remains a small effect of the total flow change on the MSB/DTG that is obscure in Fig. 2(c). To evaluate quantitatively this residual effect, we measured the mass-change rates under three different flow control conditions as follows: (i) total flow rate was maintained at 1 L/min, (ii) maintained at 20 L/min, and (iii) changed alternately between 1 L/min and 20 L/min at intervals of 2 h in a manner similar to that shown in Fig. 2(a). The mass-change rates were determined using least-squares analysis. The measurement time was approximately 22 h. The number of measurements under each flow control condition was ten. The results of the measurements are graphically shown in Fig. 3. The numerically obtained values of the results are summarized in Table 1. No difference was observed in the average evaporation rate among the three cases in the present study. However, the standard deviation of the evaporation rate in case (iii) was larger than in the other two cases. The total flow rate was unchanged during the measurements in the other two cases. Hence, the difference in the standard deviation between cases (iii) and (i) or (ii) probably originated in the residual effect of the total flow change. It was found that the fluctuation of pressure inside the chamber observed in case (iii) was larger than in the other two cases. This fluctuation would have influenced the buoyancy acting on the diffusion cell, and as a result the measurement of the evaporation rate was affected. Therefore, the residual effect observed is probably compensated by applying buoyancy correction to the mass data. The "real mass" of the diffusion cell m

Table 1
Numerical values of evaporation rates

Case	Average evaporation rate ($\mu g\,h^{-1}$)	Standard deviation ($\mu g\,h^{-1}$)
(i)	11.50	0.30
(ii)	11.50	0.23
(iii)	11.50	0.57

Table 2
Values used for buoyancy correction

Symbol	Value and unit
ρ	7.374 g/cm^3
ρ_0	8.000 g/cm^3
M_a	28.96 g/mol
M_g	28.01 g/mol
M_w	18.02 g/mol
R	8.314 J/(mol K)

is calculated with the MSB reading r, air density ρ_a, the density of the inside gas ρ_g, the density of the diffusion cell ρ, and density of the reference weight (for balance calibration) ρ_0, using the following relation:

$$m = r\frac{1-\rho_a/\rho_0}{1-\rho_g/\rho}. \quad (1)$$

Under the conditions in the present study, the water vapor and N_2 gas can be approximated to be ideal. When P_a is the atmospheric pressure, T the room temperature, and h_r is the relative humidity (in %), the air density ρ_a is approximately given by [12,13]

$$\rho_a = \frac{P_a M_a}{RT}\left[1-\frac{e_s(T)h_r}{100P_a}\left(1-\frac{M_w}{M_a}\right)\right], \quad (2)$$

where R is the molar gas constant, $e_s(T)$ the saturation vapor pressure of water at T, M_a the molar mass of dry air, and M_w is the molar mass of water. Similarly, when P_g and T_g represent the pressure and temperature of the gas inside the chamber, respectively, the density of the inside gas ρ_g is approximately given by

$$\rho_g = \frac{P_g M_g}{RT_g}, \quad (3)$$

where M_g is the molar mass of the N_2 gas. The relationship between the saturation vapor pressure of water and temperature is given by Eq. (2) in Ref. [14]. Buoyancy-corrected mass data were obtained using Eqs. (1)–(3) and Eq. (2) in Ref. [14] with the values shown in Table 2. The evaporation rates redetermined using these data are graphically shown in Fig. 4. Using

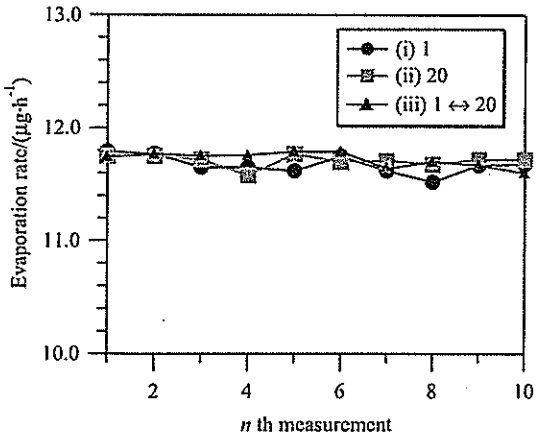

Fig. 4. Buoyancy-corrected mass-change rates. The symbols are the same as those in Fig. 3.

Table 3
Numerical values of evaporation rates (buoyancy corrected)

Case	Average evaporation rate ($\mu g\,h^{-1}$)	Standard deviation ($\mu g\,h^{-1}$)
(i)	11.67	0.08
(ii)	11.71	0.05
(iii)	11.72	0.07

numerical data corresponding to these evaporation rates, their averages and standard deviations for the three cases are calculated as summarized in Table 3. The residual effect observed in case (iii) is greatly reduced, as expected, and all the standard deviations are comparable. Moreover, the mean value of the standard deviations becomes approximately six times smaller than that obtained from Table 1. We performed an analysis of variance [11] on these data. The results of the analysis showed no significant effect due to the change in the total flow rate at a confidence level of 95%. Therefore, we do not further consider the uncertainty due to the total flow change.

3.2. Uncertainty of flow rate

In this section, we evaluate the uncertainty of the total flow rate in the system. Fig. 5 shows the relative standard deviation of the flow rate, obtained from the flow measurement with the MFMs at eight set values of MFC_1 in the range between 1.0 L/min and 20.0 L/min. This quantity corresponds to the relative standard uncertainty of the flow stability u_{fs}. The number of measurements at each set value was four or five, and the measurement time of each experiment was approximately 22 h. In Fig. 5, the instability rapidly increased with decreasing the total flow rate. This was because the MFC with a large full scale (20 L/min) was used for the flow control even in a small range. However, the observed u_{fs} was less than 0.15% in the entire range, and it was considered to be satisfactorily stable for the purpose of the present study because it was smaller than the relative standard uncertainty of the stability of trace-moisture generation, 0.6% [3].

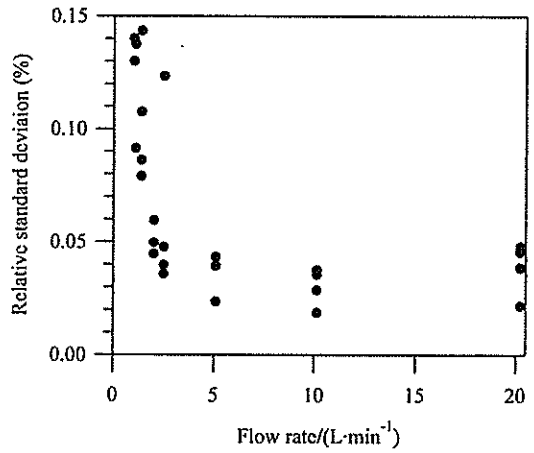

Fig. 5. Relative standard deviation of flow rate obtained from flow measurement with MFMs.

Table 4
Relative standard uncertainty

Quantity	Uncertainty component	Type	Relative standard uncertainty (%)
Humidity (x_w)	Flow rate (u_{fm})		(0.17–0.22)
	Calibration of MFM (u_{fc})	B	0.17 and 0.18
	Stability of MFM reading (u_{fs})	A	0.019–0.15
	Long-term drift (u_{fl})	B	0.015
	Evaporation rate		(0.96–1.3)
	Calibration of balance	B	0.0016
	Line fitting	A	0.084–0.14
	Stability of weighing system	A	0.75–1.2
	Buoyancy correction	B	0.021–0.11
	Temperature effect on scale interval of balance	A	0.29–0.69
	Stability of evaporation rate	A	0.16–0.35
	Residual moisture	B	0.12–2.4
	Total		1.0–2.7
Humidity (x_{ma})	Calibration of MA	B	2.3
	Stability of MA reading	A	0.35–2.6
	Total		2.3–3.5

The relative standard uncertainty of flow measurement u_{fm} is given by

$$u_{fm} = \sqrt{u_{fs}^2 + u_{fc}^2 + u_{fl}^2}, \quad (4)$$

where u_{fc} and u_{fl} represent the relative standard uncertainty due to the calibration of the MFM and due to the long-term drift, respectively. In this work, the calibration was performed using the Japan Calibration Service System (JCSS), through which the traceability to the national standard was guaranteed. The relative standard uncertainty of the flow rate between 1 L/min and 20 L/min in this system is given in Table 4. All the experiments were completed within 6 months after the calibration, and u_{fl} was estimated under the conditions of normal use for 1 year [15]. Types A and B in Table 4 express uncertainty components evaluated by statistical methods and those evaluated by other means, respectively [11]. In this work, we improved the uncertainty of the flow rate to be 0.17–0.22%; it was 2.9% in Ref. [3].

It is interesting to point out that the uncertainty was less than or equal to 0.22% although the uncertainty of the MFC_1 reading, u_{mfc}, reported by the manufacturer, was 0.58–12%; u_{fm} is smaller than u_{mfc}, even though MFC_1 was a main component of the system for the flow control. This contradiction is explained by the assumption that u_{mfc} includes the uncertainty due to the long-term drift evaluated in terms of the time scale of years that is not necessarily required for an uncertainty analysis when the reading of an MFC has been calibrated recently and the measurement is completed within a few months. MFC_1 was calibrated 5 years ago. Therefore, the long-term drift should be considered if the flow rate is determined only from the reading of MFC_1. In fact, the reading of MFC_1 deviated greatly from the MFM reading, by 0.23% to 4.3%, and the expanded uncertainty [11] of MFC_1 calculated using $2u_{mfc}$ (≈95% confidence level) covered all those deviations. The reproducibility of the flow control with MFC_1 was also estimated using the MFMs. MFC_1 had been turned on during the entire experimental period (approximately 1 month) to avoid any kind of drift derived from the switching. The flow rates observed at a set value of MFC_1 were reproduced within the uncertainty of 0.12% in the present work. This was also smaller than $2u_{mfc}$. These facts suggest that a large part of the uncertainty of an MFC is probably attributable to long-term drift; a smaller uncertainty of an MFC reading than that stated by the manufacturer may be realized by calibrating it at an appropriate interval in a proper way.

3.3. Comparison with MA measurement

Using the evaporation rate measured at the same time as in the flow measurements described in Section 3.2, we determined the humidity generated with the MSB/DTG, in amount-of-substance fraction, denoted by x_w. The evaporation rate was calculated using buoyancy-corrected data. The generated humidity was also monitored with the MA, denoted by x_{ma}. These results are summarized in Table 5, where the number following the symbol ± denotes the expanded uncertainty with a coverage factor $k=2$ (≈95% confidence level) in the unit of the quoted result. x_w was varied in the

Table 5
Comparison between generated and measured values[a]

x_w (nmol/mol)	x_{ma} (nmol/mol)	x_{ma}/x_w
247.3 ± 4.9	234.4 ± 11.0	0.95
218.4 ± 5.5	208.6 ± 9.8	0.96
171.5 ± 4.7	163.3 ± 7.7	0.95
122.3 ± 2.8	116.1 ± 5.5	0.95
95.0 ± 2.6	90.5 ± 4.3	0.95
48.1 ± 1.1	46.1 ± 2.2	0.96
24.2 ± 0.8	23.3 ± 1.2	0.96
12.2 ± 0.7	11.8 ± 0.8	0.97

[a] The numbers following the symbol ± denote the expanded uncertainty with a coverage factor $k=2$.

range of 10–250 nmol/mol; x_{ma} was consistent with x_w. The uncertainties in Table 5 were tentatively estimated similarly to that described in Ref. [3]. The uncertainty components other than flow rate considered in the analysis are listed in Table 4. The uncertainty of the evaporation rate was greatly improved to be 0.96–1.3%, compared with 0.7–8.9% in the previous work. We performed buoyancy correction on the mass data, and compensated for the uncertainty due to the buoyancy effect. Thus, this uncertainty was considered negligible in this work. Instead, we considered uncertainty due to an incomplete knowledge of the required value of the buoyancy correction, which was estimated using the calibration uncertainties of the thermometers, pressure sensors, and humidity sensor. This uncertainty was approximately two orders of magnitude smaller than the value of the buoyancy correction. The scale interval of the balance depends slightly on the ambient temperature, and the change in the interval due to the temperature fluctuation becomes an uncertainty component of evaporation rate. This effect can be reduced by calibrating the balance using an internal weight. In this work, the balance was calibrated every 30 min, instead of every 2 h, which is in contrast to the previous work, leading to a smaller uncertainty than that in Ref. [3]. With all these improvements, we have achieved uncertainties in x_w approximately twice as small as those in Ref. [3] in the range of 20–250 nmol/mol. Furthermore, in this work, we have expanded the range of trace-moisture generation down to 12.2 nmol/mol with an expanded uncertainty of 0.7 nmol/mol ($k=2$).

In the previous study, deviation was observed between x_w and x_{ma}, which we attributed to systematic errors in the readings of the MFC and MA. The deviation was also observed in this study. x_{ma} was biased 3–5% lower than x_w, as shown in Table 5 (x_{ma}/x_w), although the bias due to the flow measurement in this study was estimated to be 0.36% ($=2u_{fc}$) at maximum. Therefore, we concluded that the deviation was mainly attributable to the systematic errors in the MA reading. Let N_w and N_g represent the number densities of water and the total gas, respectively. These quantities are related to the MA reading x_{ma} by

$$x_{ma} = \frac{N_w}{N_g}. \tag{5}$$

N_w can be calculated from the two measured ring-down times [6] τ and τ_0 at the line center position ν_0, where τ is the ring-down time for the cavity containing the trace-moisture gas and τ_0 is the ring-down time for the cavity containing only the dry gas. If the absorption cross section of water σ is known, N_w is determined using [6]:

$$N_w = \frac{1}{c\sigma(\nu_0)}\left(\frac{1}{\tau(\nu_0)} - \frac{1}{\tau_0(\nu_0)}\right) \equiv \frac{1}{c\sigma(\nu_0)}L(\nu_0), \tag{6}$$

where c is the speed of light in the medium within the cavity. The absorption cross section for a single absorption line can be written in the form

$$\sigma(\nu) = S(T)f(\nu - \nu_0), \tag{7}$$

where $S(T)$ is the line strength at temperature T and f is the normalized line-shape function. Because the MA uses a Lorentz function for the line shape [16], the absorption cross section at the line center is given by [17]

$$\sigma(\nu_0) = \frac{S(T)}{\pi b_L}, \tag{8}$$

where b_L expresses the Lorentz half width. In the present study, the pressure broadening due to H_2O–H_2O collisions is negligible because the concentration of water is extremely low. Therefore, b_L is approximated by

$$b_L = \gamma(T)P, \tag{9}$$

where γ is the broadening coefficient of H_2O by N_2 at temperature T, and P is the pressure of the total gas. N_g is given by

$$N_g = \frac{P}{kT}, \tag{10}$$

where k represents the Boltzmann constant. From Eqs. (5)–(10), the MA reading is given by

$$x_{ma} = \frac{\pi\gamma(T)kT}{cS(T)}L(\nu_0). \tag{11}$$

Using this equation, we discuss three sources presumably responsible for the bias observed in the present study.

First, the MA measures only $L(\nu_0)$ in Eq. (11), and x_{ma} is calculated on the basis of T/K = 296 [16]. However, in the present study, the temperature of the absorption cell was estimated to be 304 K. The line strength $S(T)$ is related to the strength S_0 at a reference temperature T_0 by [18]

$$S(T) = S_0\left(\frac{T_0}{T}\right)^{1.5}\exp\left[-\frac{hcE_0}{k}\left(\frac{1}{T} - \frac{1}{T_0}\right)\right], \tag{12}$$

where h is the Planck constant and E_0 is the lower level energy expressed in cm^{-1}. The MA monitors the $2_{02} \leftarrow 3_{03}$ transition of the $\nu_1 + \nu_3$ band of H_2O at 7181.156 cm^{-1}, therefore, $E_0 = 136.76\,cm^{-1}$ [19]. The broadening coefficient $\gamma(T)$ is expressed as

$$\gamma(T) = \gamma_0\left(\frac{T_0}{T}\right)^n, \tag{13}$$

where γ_0 is the coefficient at T_0 and $n = 0.73$ for the line [19]. Substituting Eqs. (12) and (13) into Eq. (11), we can calculate the ratio of $x_{ma}(T/K = 296)/x_{ma}(T/K = 304)$ to be 0.971. This suggests that x_{ma} in this work is 3% lower than x_w.

Second, the uncertainty of the line strength should be considered. The values of S_0 for the line reported in literature differed at maximum by 6% [20], indicating the difficulty in determining the value with a relative uncertainty much less than ~3%. The inaccuracy in S_0 results in a systematic error in x_{ma}. Eq. (11) shows that the overestimation of S_0 leads to the underestimation of x_{ma}. Although the numerical value of S_0 for the MA reading is unreported, the observation implies that an overestimated value is likely to be used.

Finally, the choice of the line-shape function may also affect x_{ma}. Lisak et al. have recently investigated rovibrational H_2O spectra using some line-shape models in the pressure range

below 60 kPa [21]. They reported that the differences in the line strengths determined using various line-shape functions could be significant, varying in some cases by more than a few percent. However, it is unclear to what extent this effect contributed to x_{ma}, because they did not use a Lorentz function for the analysis and the pressure inside the absorption cell of the MA in this work ($\geq$140 kPa) differed from that used in their study.

Note that the bias due to the effects mentioned above can be compensated by measuring the temperature of the gas and by calibrating the MA reading using a reliable humidity standard.

4. Conclusions

We have developed a system of flow and pressure controls for the MSB/DTG to realize a humidity standard in the trace-moisture region. The amount-of-substance fraction of water in the trace-moisture gas generated with the DTG can easily be varied and controlled using the system. It has been demonstrated that buoyancy correction is an effective method of reducing the uncertainty of evaporation rates measured with the MSB. Using the system and buoyancy-corrected data, the negative effect on the MSB/DTG observed upon changing the total flow rate become negligible. We evaluated the relative standard uncertainty of the total flow rates to be less than or equal to 0.22% using mass flow meters composed of critical flow Venturi nozzles. It is suggested that a smaller uncertainty of an MFC reading than that stated by the manufacturer may be realized by calibrating it at an appropriate interval in a proper way. With the improvements introduced in this work, we have achieved uncertainties in x_w approximately twice as small as those in the previous work. Furthermore, we have expanded the range of the trace-moisture generation down to 12 nmol/mol. A comparison between the humidity determined using the evaporation and flow rates and that measured with the MA was presented. These two values were consistent. The MA reading was determined on the basis of spectroscopic measurement, independent of any humidity measurement using the MSB and MFMs. Therefore, the results of the comparison also confirm that the DTG is capable of producing a trace-moisture gas down to approximately 10 nmol/mol, and of varying and controlling the amount-of-substance fraction of water using the system developed in this work. The sources of the bias observed in the MA reading are attributable mainly to systematic errors in the temperature of the absorption cell and absorption cross section used to calculate the water concentration with the MA. This bias can be compensated by measuring the temperature of the gas and by calibrating the MA reading.

Acknowledgements

We would like to thank Dr. Shin-ichi Nakao for helpful comments on the flow measurement, and Dr. Chiharu Takahashi and Dr. Nobuaki Ochi for critically reading the manuscript. We are also grateful to Dr. Wen-Bin Yan (Tiger Optics) for providing us with valuable information on the MA, and to Takeshi Yakuwa (Hirai) for useful comments on the uncertainty analysis of the MFM measurement.

References

[1] International Technology Roadmap for Semiconductors, 2004.
[2] H.H. Funke, B.L. Grissom, C.E. McGrew, M.W. Raynor, Techniques for the measurement of trace moisture in high-purity electronic specialty gases, Rev. Sci. Instrum. 74 (2003) 3909–3933.
[3] H. Abe, H. Kitano, Development of humidity standard in trace-moisture region: characteristics of humidity generation of diffusion tube humidity generator, Sens. Actuators A 128 (2006) 202–208.
[4] A. O'Keefe, D.A.G. Deacon, Cavity ring-down optical spectrometer for absorption measurements using pulsed laser sources, Rev. Sci. Instrum. 59 (1988) 2544–2551.
[5] D. Romanini, K.K. Lehmann, Ring-down cavity absorption spectroscopy of the very weak HCN overtone bands with six, seven, and eight stretching quanta, J. Chem. Phys. 99 (1993) 6287–6301.
[6] G. Berden, R. Peeters, G. Meijer, Cavity ring-down spectroscopy: experimental schemes and applications, Int. Rev. Phys. Chem. 19 (2000) 565–607.
[7] J.D. Wright, G.E. Mattingly, S. Nakao, Y. Yokoi, M. Takamoto, International comparison of a NIST primary standard with an NRLM transfer standard for small mass flow rates of nitrogen gas, Metrologia 35 (1998) 211–221.
[8] S. Nakao, Y. Yokoi, M. Takamoto, Development of a calibration facility for small mass flow rates of gas and the uncertainty of a sonic venturi transfer standard, Flow Meas. Instrum. 7 (1996) 77–83.
[9] M. Hayakawa, Y. Ina, Y. Yokoi, M. Takamoto, S. Nakao, Development of a transfer standard with sonic Venturi nozzles for small mass flow rates of gases, Flow Meas. Instrum. 11 (2000) 279–283.
[10] N. Bignell, Using small sonic nozzles as secondary flow standards, Flow Meas. Instrum. 11 (2000) 329–337.
[11] ISO, Guide to the expression of uncertainty in measurement, 1995.
[12] P. Giacomo, Equation for the determination of the density of moist air (1981), Metrologia 18 (1982) 33–40.
[13] R.S. Davis, Equation for the determination of the density of moist air (1981/91), Metrologia 29 (1992) 67–70.
[14] D. Sonntag, Important new values of the physical constants of 1986, vapor pressure formulations based on the ITS-90, and psychrometer formulae, Z. Meteorol. 70 (1990) 340–344.
[15] T. Yakuwa, private communication.
[16] W.-B. Yan, private communication.
[17] M.A.H. Smith, C.P. Rinsland, B. Fridovich, K.N. Rao, in: K.N. Rao (Ed.), Molecular Spectroscopy: Modern Research, vol. III, Academic Press, Orlando, 1985, pp. 111–248 (Chapter 3).
[18] B. Parvitte, V. Zéninari, I. Pouchet, G. Durry, Diode laser spectroscopy of H_2O in the 7165–7185 cm^{-1} range for atmospheric applications, J. Quant. Spectrosc. Radiat. Transfer 75 (2002) 493–505.
[19] C. Delaye, J.-M. Hartmann, J. Taine, Calculated tabulations of H_2O line broadening by H_2O, N_2, O_2, and CO_2 at high temperature, Appl. Opt. 28 (1989) 5080–5087.
[20] R.A. Toth, Measurements of positions, strengths and self-broadened widths of H_2O from 2900 to 8000 cm^{-1}: line strength analysis of the 2nd triad bands, J. Quant. Spectrosc. Radiat. Transfer 94 (2005) 51–107.
[21] D. Lisak, J.T. Hodges, R. Ciurylo, Comparison of semiclassical line-shape models to rovibrational H_2O spectra measured by frequency-stabilized cavity ring-down spectroscopy, Phys. Rev. A 73 (2006) 012507.

Biographies

Hisashi Abe received his PhD degree in physics in 1996 from Kanazawa University, Japan. He is a researcher at the National Metrology Institute of Japan (NMIJ).

Hiroshi Kitano received his MS degree in chemistry in 1977 from Osaka University, Japan. He is the chief of the Humidity Standards Section at the NMIJ.